Polymer 50 (2009) 6305–6311

Contents lists available at ScienceDirect

Polymer

journal homepage: www.elsevier.com/locate/polymer

# Temperature dependent microphase mixing of model polyurethanes with different intersegment compatibilities

Suphannee Pongkitwitoon [a], Rebeca Hernández [b], Jadwiga Weksler [c], Ajay Padsalgikar [c], Taeyi Choi [a], James Runt [a,*]

[a] Department of Materials Science and Engineering, The Pennsylvania State University, University Park, PA 16802, USA
[b] Instituto de Ciencia y Tecnología de Polímeros, CSIC, Juan de la Cierva, 328006 Madrid, Spain
[c] AorTech Biomaterials, Dalmore Drive, Caribbean Park, Scoresby, VIC 3179, Australia

## ARTICLE INFO

*Article history:*
Received 14 August 2009
Received in revised form
19 October 2009
Accepted 29 October 2009
Available online 5 November 2009

*Keywords:*
Segmented polyurethane copolymers
Microphase separation
Synchrotron small-angle X-ray scattering

## ABSTRACT

In this paper we explore the temperature dependence of segregation of hard and soft segments of selected segmented polyurethane copolymers using synchrotron small-angle X-ray scattering (SAXS). The copolymers are composed of the same hard segments but three different soft segment chemistries, of particular interest in biomedical device applications. Hard segments are formed from 4,4′-methylenediphenyl diisocyanate and 1,4-butanediol, and soft segments from an aliphatic polycarbonate [poly(1,6-hexyl 1,2-ethyl carbonate)], poly(tetramethylenoxide), or a mixed soft segment synthesized from hydroxyl-terminated poly(dimethylsiloxane) [PDMS] and poly(hexamethylenoxide) macrodiols. The changes in SAXS relative invariants and interdomain spacings are indicative of gradual dissolution of phase separated hard and soft segments with increasing temperature. All copolymers investigated herein, even those containing PDMS soft segments, transform to the single-phase state at a temperature determined by the soft segment chemistry (and hard segment content). The SAXS findings, along with those from parallel temperature-controlled Fourier Transform infrared spectroscopy measurements, also facilitate assignment of the origin of the thermal events observed in the DSC thermograms of these materials.

## 1. Introduction

Segmented polyurethane (PU) copolymers are used extensively in applications ranging from foams and coatings, to a variety of important applications in life-saving biomedical devices. These polymers can be synthesized from a wide variety of isocyanates, diol or diamine chain extenders, and polyols, using convenient addition polymerization methods. However, although the polyol (i.e., the precursor for the low $T_g$ soft segments) has a relatively well-defined molecular weight, the nature of the polymerization generally yields 'hard' segments with a rather broad distribution of sequence lengths [1]. This creates complexity in understanding segmented PU microphase separation compared to diblock and triblock copolymers, in which the blocks have well-defined lengths and narrow polydispersity.

PUs having different soft segment chemistries commonly exhibit rather incomplete hard/soft demixing when polymerized in the bulk or cast from solution, and the extent of unlike segment segregation (and resulting hard domain morphology) is particularly important in determining mechanical and other physical properties [2–4]. This arises from several factors. Hard segments having short sequence lengths (as well as so-called 'lone' isocyanates [5], more prevalent at lower hard segment contents), have greater solubility in the soft phase than longer sequences for entropic reasons [6]. In addition, similarity in cohesive energy density and/or the possibility of hydrogen bonding between hard and soft repeat units also encourage mixing. This is illustrated in some of our earlier work in which we compared degrees of hard/soft segment phase separation, quantitatively determined from small-angle X-ray (SAXS) experiments, for model PUs having the same hard segments [4,4′-methylenediphenyl diisocyanate (MDI) chain extended with 1,4-butanediol (BDO)] and hard segment contents, and 1000 Da soft segments composed of poly(tetramethylenoxide) [PTMO], poly(1,6-hexyl 1,2-ethyl carbonate) [PHEC] or soft segments composed predominately of PDMS [7–9]. At room temperature, the non-polar PDMS segments are completely segregated from the other components in the copolymers, while less than ~40% of the hard and soft segments are demixed in the PTMO soft segment PUs.

---

[*] Corresponding author.
*E-mail address:* runt@matse.psu.edu (J. Runt).

0032-3861/$ – see front matter © 2009 Elsevier Ltd. All rights reserved.
doi:10.1016/j.polymer.2009.10.067

PHEC forms hydrogen bonds with the hard segments and considerably less (ca. 10–15%) of the hard and soft segments are segregated for these copolymers.

Demixing kinetics (relative to polymerization or solvent casting time scales and thermal history) also plays a critical role in determining the ultimate degree of segment segregation, in some cases limiting it to values considerably below what one would anticipate under nominally equilibrium conditions [10]. Degrees of hard/soft segment segregation are also strongly influenced by temperature, as demonstrated previously for various polyether soft segment PUs by synchrotron SAXS experiments [11–13].

In the current paper, we report on our continuing investigation of PUs synthesized with PTMO, PHEC and PDMS – based soft segments, turning now to the temperature dependence of the phase behavior. This is of importance in understanding mechanical performance at elevated temperatures and to establishing minimum processing temperatures by identifying the temperature at which complete hard/soft segment mixing occurs (defined here as the microphase mixing temperature, $T_{\mathrm{MMT}}$). We use synchrotron SAXS to follow the gradual hard/soft segment mixing as a function of temperature and perform parallel temperature-controlled Fourier Transform infrared (FTIR) spectroscopy experiments that provide insight into hard segment hydrogen bonding. DSC thermograms of the copolymers were also acquired and the thermal events interpreted in light of the SAXS findings.

Although there have been some previous reports on the temperature dependence of the phase behavior of PUs with some different polyether – based soft segments [14–18], this is the first report for PUs synthesized with PHEC and PDMS – based soft segment chemistries, of keen interest for emerging biomedical devices. One initially surprising finding is that, although non-polar PDMS segments are completely segregated from the remaining units at room temperature, they dissolve in the chemically dissimilar hard (and polyether) segments at elevated temperatures, the precise value depending on the hard segment content.

## 2. Experimental section

### 2.1. Materials

The hard segment chemistry of the PU copolymers under investigation here is based on MDI and BDO [purchased from Sigma Aldrich (98% purity)] and have 40 wt% hard segments. Three different macrodiols were used to create soft segments: a poly(tetramethyleneoxide) diol ($M_w = 1000$, obtained from Urethane Compounds), a poly(1,6-hexyl 1,2-ethyl carbonate) diol ($M_w = 1000$, obtained from UBE Industries), and a mixed macrodiol composed of hydroxyterminated poly(dimethylsiloxane) ($M_w = 1000$) and poly(hexamethylenoxide) [PHMO] diol ($M_w = 700$) [both synthesized by AorTech Biomaterials], in a ratio of 80/20 w/w. The polydispersity of the macrodiols was ~1.5 and purities were all >97%. The hydroxyterminated poly(dimethylsiloxane) was subjected to thorough fractional distillation on a thin film evaporator. The distilled material was evaluated using gas chromatography to ensure that all low molecular weight cyclics were removed. Details of the chemical structure of each of the considered soft segments are provided in Fig. 1.

PUs were synthesized via a two-step process. In general, a prepolymer was prepared by carefully adding MDI to a reaction vessel containing the appropriate macrodiol and BDO was subsequently added for chain extension. PTMO and PDMS/PHMO copolymers were synthesized using a bulk procedure [19] while the PHEC copolymer was synthesized in solution in *N*,*N* dimethylacetamide (DMAc, LC grade, 99%, Biolab Australia, minimum 99% purity). The principle reason that the PHEC based materials were solution polymerized was to follow the same two-step addition scheme. Without a solvent, we could not prepare the PHEC–PUs using a two-step process. Once the solvent is removed, the PHEC–PU was melt-processable. Materials are denoted as PTMO-40, PDMS/PHMO-40 and PHEC-40 and have number average molecular weights of 149 600, 170 900 and 62 800 Da, respectively. Molecular weights were determined by gel permeation chromatography using DMF (with 0.05 M LiBr) as the mobile phase, relative to polystyrene standards.

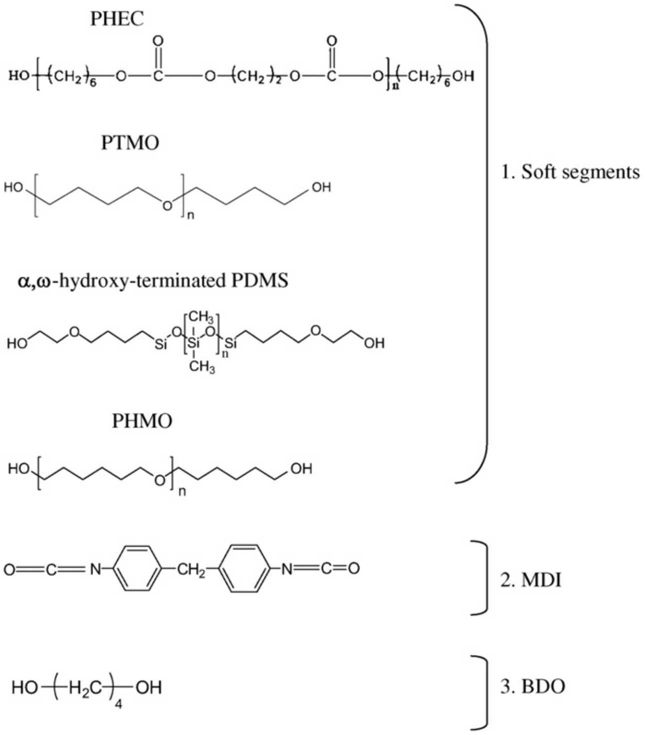

**Fig. 1.** Chemical structures of the components of three polyurethanes under consideration.

### 2.2. Differential scanning calorimetry

Phase transitions of the copolymers were determined using a TA-Q1000 DSC. Each sample was first cooled to −90 °C and heated at a rate of 10 °C/min up to 250 °C.

### 2.3. Temperature-controlled FTIR spectroscopy

Temperature-controlled transmission FTIR spectroscopy was conducted using a Nicolet 6700 FTIR (Thermo Scientific). PTMO-40, PDMS/PHMO-40 and PHEC-40 were dissolved in DMAc (2 wt% PU) and the solutions were cast onto KBr windows. Specimens were dried overnight under ambient conditions and further dried for 2 h at 80 °C under vacuum. Samples were scanned 100 times at a resolution of 2 $\mathrm{cm}^{-1}$ from 30 °C to 150 °C (or 180 °C for PDMS/PHMO-40) in 10 °C increments of ~ 3 °C/min.

### 2.4. Synchrotron small-angle X-ray scattering

Synchrotron SAXS was carried out at the Stanford Synchrotron Linear Accelerator Center. The X-ray wavelength ($\lambda = 1.5488$ Å) was controlled within an error ($d\lambda/\lambda \sim 1\%$) and was configured by focusing independently in the horizontal and vertical planes, leading to a beam size of ~0.2 mm diameter. The sample-to-detector distance was 1.34 m, corresponding to an available scattering vector range of $0.1 < q\ (\mathrm{nm}^{-1}) < 2.0$. The two dimensional scattering was radially averaged to yield one-dimensional scattering profiles. The data were corrected for dark count and background noise, then normalized by sample thickness. The scattering vector was calibrated using silver behenate.

Sample films ($\sim$1 mm thick) were cut into 1 cm × 1 cm squares, placed in an aluminum sample cell and then sealed. Samples were heated from 30 °C to 220 °C at a rate of 10 °C/min with controlled temperature precision (within ±1 °C).

### 2.5. Data analysis

The scattering intensity, $I(q)$, is displayed as a function of scattering vector, $q = 4\pi\ \sin\theta/\lambda$, where $2\theta$ is the scattering angle. The $q$ value at which the scattered intensity is a maximum ($q_{\max}$) reflects the mean spacing ($d$) between hard domains ($d = 2\pi/q_{\max}$). The invariant, $Q$, is the total scattered intensity:

$$Q = \int_0^{\infty} I(q)q^2\mathrm{d}q \tag{1}$$

For an ideal two-phase system with sharp interfaces, $Q$ can be written as:

$$Q = 2\pi^2\left[\phi_1(1-\phi_1)(\eta_2-\eta_1)^2\right] \tag{2}$$

where $\phi_i$ is the volume fraction and $\eta_i$ the electron density of the $i$th phase.

When investigating temperature dependent SAXS, it is necessary to take into consideration that the difference between the thermal expansion coefficients of the two phases may lead to a change in $(\eta_2-\eta_1)^2$ and therefore influence the measured $Q$. The thermal expansion coefficient (CTE), $\alpha$, is defined as $\partial\eta/\partial T$. Then by means of Eq. (2) it can be shown that if the volume fractions of the phases remains relatively constant, the following expression can be written for $Q(T)$ [20,21].

$$\left[\frac{Q_T}{Q_{T_0}}\right]^{1/2} = 1 + \frac{(\alpha_1-\alpha_2)}{|\eta_{1(T_0)}-\eta_{2(T_0)}|}(T-T_0) \tag{3}$$

where $T_0$ is a reference temperature and $\alpha_1$ and $\alpha_2$ are the thermal expansion coefficients of phases 1 and 2, respectively.

## 3. Results and discussion

For perspective on the findings that follow, we first provide some salient room temperature characteristics of the segmented PUs under consideration. The PTMO and PHEC PUs (with 1000 Da soft segment molecular weight) exhibit a typical two-phase microstructure of hard domains in a soft matrix. Evidence from our previous studies and elsewhere suggests that the hard domains consist principally of hard segments, while the soft phase consists of soft segments and some dissolved or trapped hard segments. Tapping mode atomic force microscopy experiments demonstrate for all of our model PUs that the hard domains are discrete and have a diameter of ca 10 nm [8]. As noted earlier, neither of these series of copolymers (over the range of hard segment contents investigated) exhibit high degrees of hard/soft segment segregation (as defined by quantitative SAXS experiments): the PTMO PUs (with ≤45 wt% hard segments) exhibit degrees of hard/soft segment demixing of 30–35%, while the PHEC PUs exhibit much smaller values of 10–15% as a result of hydrogen bonding between hard and soft segments [8].

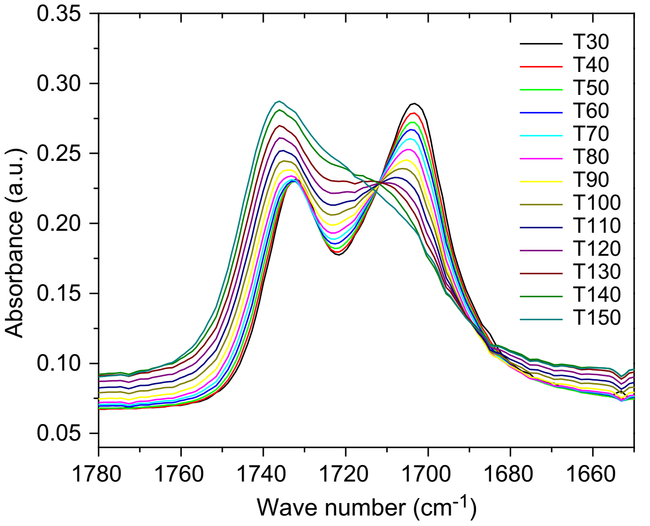

**Fig. 2.** FTIR spectra from 1800 to 1650 $\mathrm{cm}^{-1}$ as a function of temperature for PTMO-40.

However, copolymers synthesized with mixed soft segments of hydroxyterminated poly(dimethylsiloxane) and poly(hexamethylenoxide) diol or only hydroxyterminated PDMS [22] organize into *three phases*: hard domains, domains consisting of siloxane units only, and a mixed phase composed of PHMO, PDMS-end group segments, and dissolved hard segment sequences [8,9,19,23]. The morphology of these copolymers can be considered to be core–shell like: with the hard domains serving as the core, the mixed phase as the shell, and the biostable PDMS as the matrix.

### 3.1. Temperature-controlled FTIR

The carbonyl stretching regions (1650–1780 $\mathrm{cm}^{-1}$) of the 40 wt% hard segment PU copolymers are displayed in Figs. 2–4 as a function of temperature. Curve fitting of this spectral region was performed in a manner similar to that described previously for polyurethanes [24] and polyamides [25]. For PTMO-40 and PDMS/PHMO-40, three absorbances are considered in the curve fitting: a contribution from strongly hydrogen-bonded carbonyls at

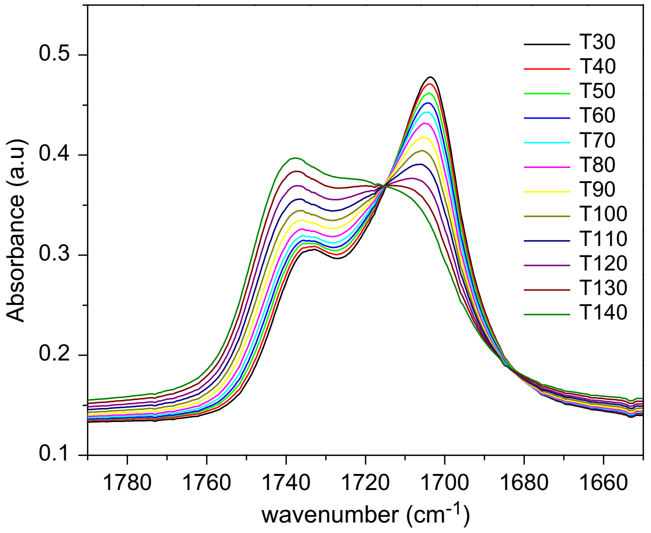

**Fig. 3.** FTIR spectra from 1800 to 1650 $\mathrm{cm}^{-1}$ as a function of temperature for PDMS/PHMO-40.

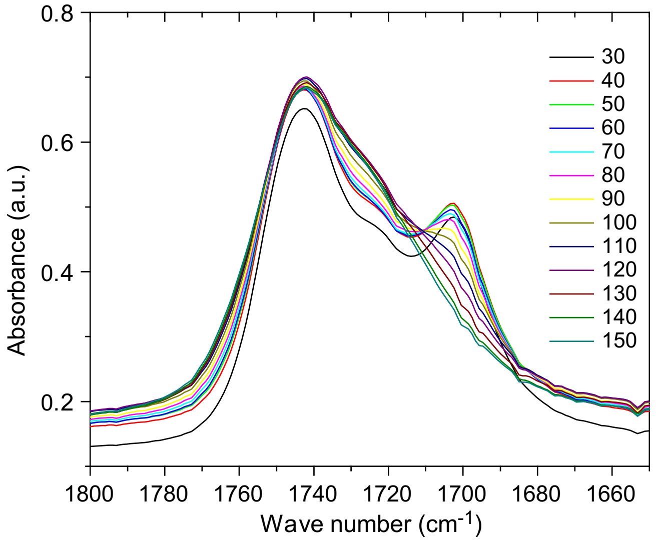

**Fig. 4.** FTIR spectra from 1800 to 1650 cm$^{-1}$ as a function of temperature for PHEC-40.

$\sim$1700 cm$^{-1}$, loosely hydrogen-bonded carbonyls (disordered hydrogen-bonded groups) at $\sim$1715 cm$^{-1}$, and free (non-hydrogen-bonded) carbonyls at $\sim$1735 cm$^{-1}$ [24,26,27]. An iterative least-squares program was used to obtain the best fit of the experimental data by varying the frequency ($\nu$), width at half height (w) and intensity (A) of three Gaussian–Lorentzian bands. For PHEC-40, however, because there are a total of five closely spaced carbonyl environments (H-bonded and non-bonded carbonate carbonyls along with the three urethane carbonyl environments) [28], we did not attempt to deconvolute the contribution of each.

Relative absorbances in the C=O region of PTMO–PU and PDMS/PHMO–PU were adjusted by taking into account the differences in absorptivity between the free and hydrogen-bonded urethane C=O. The relative absorptivity for hydrogen-bonded carbonyls for a model polyurethane was determined to be 1.71 [24]. The fraction of carbonyl groups in each environment was then determined by dividing the area corresponding to each absorbance by the total area corresponding to the carbonyl region.

The relative fractions of the three types of carbonyl groups are displayed in Fig. 5 for the PTMO-40 and PDMS/PHMO-40 copolymers. Since hydrogen-bonded urethane carbonyls are bonded with N–H groups in urethane linkages of hard segments, the absorbance from the H-bonded carbonyls is expected to correlate in a general fashion with the extent of hard domain formation. However, this must be done with care, since the sample preparation procedure for FTIR spectroscopy is somewhat different from that of the specimens used in the SAXS experiments.

Spectral changes with increasing temperature are qualitatively similar for the three copolymers but details vary between them. PTMO-40 spectra exhibit a prominent peak at 1703 cm$^{-1}$ at lower temperatures, whose absorbance gradually decreases by about a factor two at 150 °C. At the same time, the non-bonded urethane carbonyl absorbance at $\sim$1733 cm$^{-1}$ moves to slightly higher cm$^{-1}$, and the absorbance increases with increasing temperature. These changes in hard segment H-bonding are generally consistent with the SAXS results that follow in the next section, in that they indicate a greater degree of mixing between hard and soft segments at higher temperatures.

Similar behavior for the non- and H-bonded absorbances is observed for PDMS/PHMO-40. With increasing temperature, the absorbance at $\sim$1737 cm$^{-1}$ from free carbonyls moves slightly to higher wavenumber (1743 cm$^{-1}$), as does that at $\sim$1703 cm$^{-1}$ (1709 cm$^{-1}$). Both absorbance peaks also broaden somewhat at higher temperatures. The absorbance at 1714 cm$^{-1}$ from loosely H-bonded carbonyls also moves to higher cm$^{-1}$ (1727 cm$^{-1}$) at higher temperatures. Note in Fig. 5 that the fraction of loosely bonded C=Os is smaller than the others for both PTMO-40 and PDMS/PHMO-40, but their temperature dependence is different, with that of PTMO-40 and PDMS/PHMO-40 increasing and decreasing, respectively, with temperature. These results may indicate relatively subtle differences in the changing H-bonding pattern in the hard domains of each PU, but the uncertainties involved in the curve resolving are such that this remains an open question at present. There might at first glance appear to be an anomaly in the fractions of H-bonded species around 50 °C in PDMS/PHMO–PU but the uncertainty in the curve resolving together with the 'return' of the calculated fractions to the gradual change observed at other temperatures, suggests that the resolved fractions at 50 °C are within experimental uncertainty.

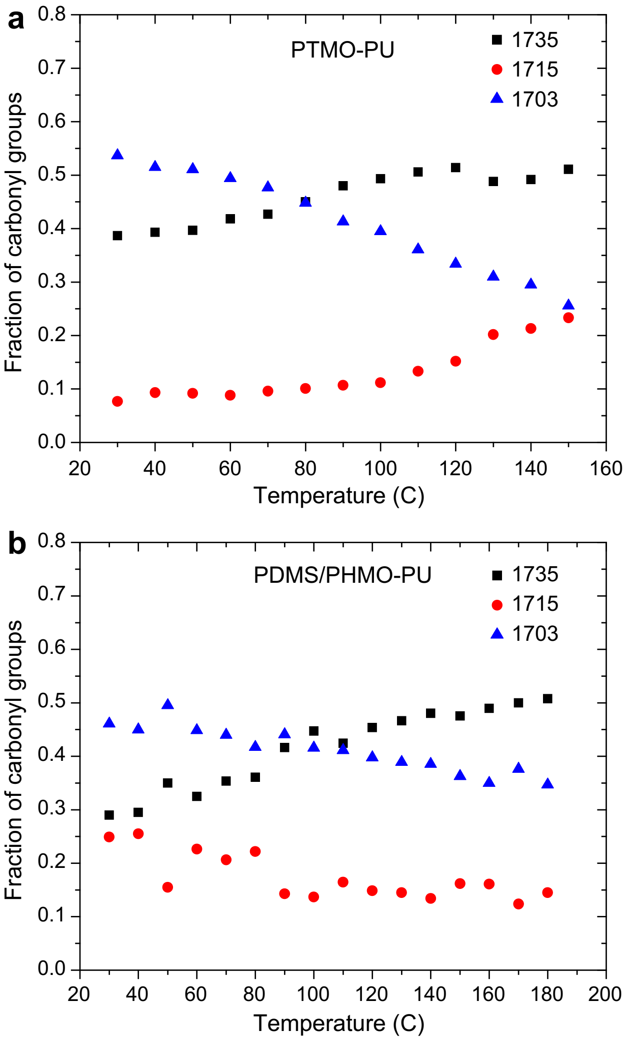

**Fig. 5.** (a) The fractions of non-bonded (■), loosely hydrogen-bonded (●) and strongly hydrogen-bonded (▲) urethane carbonyl groups for PTMO-40 in the temperature range from 30 to 150 °C, (b) The fractions of non-bonded (■), loosely hydrogen-bonded (●) and strongly hydrogen-bonded (▲) urethane carbonyl groups for PDMS/PHMO-40 in the temperature range from 30 to 180 °C.

Finally, although quantification (separation) of the carbonyl absorbances is not feasible for the PHEC-40, the strongly bonded urethane C=O absorbance located at 1702 cm$^{-1}$ does not contain a contribution from carbonate C=Os, and its relative decrease in

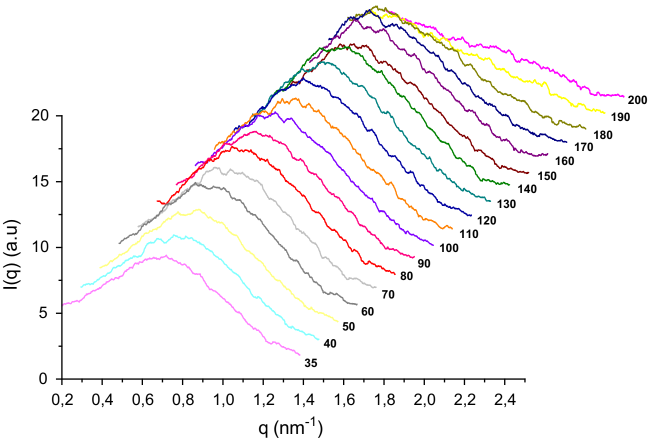

**Fig. 6.** Synchrotron SAXS scattering patterns for PDMS/PHMO-40 as a function of temperature (°C). Temperatures are noted beside the corresponding scattering curve. Each scattering curve begins at $q = 0.2\ \mathrm{nm}^{-1}$ and ends at $1.4\ \mathrm{nm}^{-1}$.

absorbance with increasing temperature is in keeping with changes in the other PU copolymers as well as the findings from SAXS experiments that are discussed below. This absorbance peak completely disappears at temperatures higher than 120 °C, which indicates mixing of the hard and soft segments, as will be corroborated in the temperature dependent SAXS presented in the next section.

### 3.2. *Temperature dependent SAXS*

Figs. 6–8 display the synchrotron SAXS profiles collected during heating for PDMS/PHMO-40, PHEC-40, and PTMO-40, respectively. For all of these materials, the invariant, *Q*, first increases modestly with increasing temperature, then decreases more significantly at higher temperatures, eventually disappearing. It is also observed that the scattering vector associated with the SAXS peak maxima shifts toward lower *q* with increasing temperature for all materials.

Evaluation of changes in *Q* requires consideration of the different thermal expansion coefficients of the hard and soft domains. The hard segment domains (MDI-BDO) are below their glass transition temperature, $T_g$ (whose precise location is uncertain, but has an upper limit of ~110 °C for long MDI-BDO segments [15]) at the lower temperatures investigated, and have a lower thermal expansion coefficient than the soft segment domains [21,29] The expansion coefficients of PHEC and PTMO were estimated using a group contribution method [30] and are approximately $1.6 \times 10^{-4}\ \mathrm{K}^{-1}$ and $6.1 \times 10^{-4}\ \mathrm{K}^{-1}$, respectively, at $T = 20$ °C. The PHEC-40 and PTMO-40 copolymers are two-phase systems but as noted earlier PDMS/PHMO-40 exhibits three phases [hard domains, a PDMS phase, and a mixed phase consisting of PHMO, polyether group segments in the PDMS – based macrodiol and some dissolved or trapped hard segments [8,9]]. However at hard segment concentrations ≥40 wt%, their small-angle X-ray scattering profiles at room temperature can be successfully modeled using a pseudo-two phase approach [9]. Following from this, we apply Eq. (2) to PDMS/PHMO-40 by considering "two phases": hard domains and another composed of siloxane units mixed with PHMO segments. As a further approximation, we consider that the siloxane units dominate the thermal expansion of the soft domains because they constitute 80 wt% of the soft segment composition. The $\alpha$ reported for PDMS in the literature is $9.1 \times 10^{-4}\ \mathrm{K}^{-1}$ [31].

Fig. 9 displays $[Q_T/Q_{T_0}]^{1/2}$ as a function of temperature for the three copolymers under investigation, where $Q_{T_0}$ is the invariant at $T_0 = 35$ °C. Considering Eq. (3), *Q* is predicted to be linearly proportional to *T* if there are no structural changes taking place in the *T* range under consideration. As seen in Fig. 9, $[Q_T/Q_{T_0}]^{1/2}$ first increases and reaches a maximum around ca. 80 °C, and then

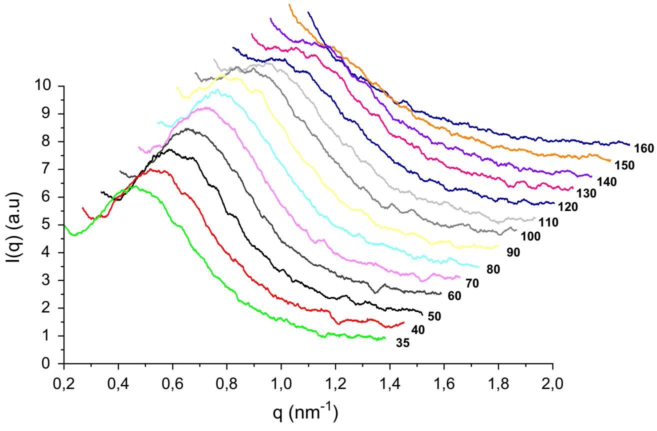

**Fig. 7.** Synchrotron SAXS scattering patterns for PHEC-40 as a function of temperature (°C). Temperatures are noted beside the corresponding scattering curve. Each scattering curve begins at $q = 0.2\ \mathrm{nm}^{-1}$ and ends at $1.4\ \mathrm{nm}^{-1}$.

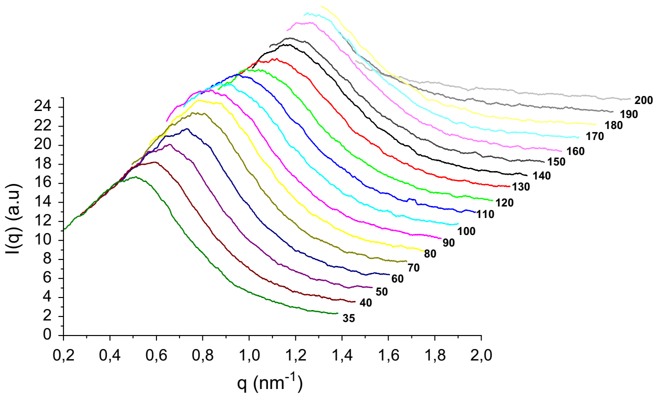

**Fig. 8.** Synchrotron SAXS scattering patterns for PTMO-40 as a function of temperature (°C). Temperatures are noted beside the corresponding scattering curve. Each scattering curve begins at $q = 0.2\ \mathrm{nm}^{-1}$ and ends at $1.4\ \mathrm{nm}^{-1}$.

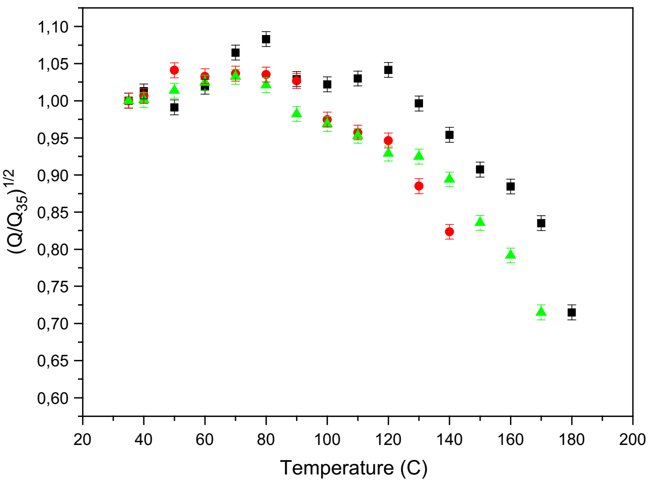

**Fig. 9.** The relative invariant $(Q_T/Q_{35C})^{1/2}$ versus temperature for PDMS/PHMO-40 (■), PTMO-40 (▲) and PHEC-40 (●).

gradually decreases. Although it is not possible to determine if the initial increase is strictly linear because of the limited number of data points, it is nevertheless reasonable to conclude that this initial increase arises from differential thermal expansion of the phases. The gradual decrease of $[Q_T/Q_{T_0}]^{1/2}$ at temperatures above ca. 80 °C for all three copolymers is indicative of the gradual dissolution of the hard domains. In fact, we very recently observed for these same PUs that the reduction in the strength of the dielectric Maxwell–Wagner–Sillars interfacial polarization, associated with the multiphase character of the PUs, parallels the gradual dissolution of the hard domains as observed in synchrotron SAXS experiments [32].

We propose that the change in relative invariant near ~80 °C is associated with the $T_g$ of the hard domains ($T_{g,H}$) since for significant dissolution of the microstructure to proceed, hard segments in hard domains must have sufficient mobility. That ~80 °C is somewhat lower than the $T_g$ of high molecular weight hard segments (MDI-BDO, 110 °C) is not surprising in that hard segment sequence lengths are rather limited in these PUs and $T_g$ is well known to be a function of molecular weight, particularly at low degrees of polymerization. $T_{g,H}$ has been notoriously difficult to locate with any certainty for many segmented PUs in DSC experiments (it has been proposed that this is because of a rather small heat capacity change associated with this transition [33]).

All copolymers transform to a single-state mixed state at elevated temperatures, and we define the order–disorder transition temperature (or microphase mixing temperature ($T_{MMT}$)), as the temperature at which the SAXS intensity completely disappears [2,11]. For PHEC-40 this occurs at ~140 °C, which is a significantly lower temperature than those observed for the PDMS/PHMO-40 and PTMO-40 copolymers (180 and 170 °C, respectively). This correlates nicely with the degrees of phase separation of three copolymers at room temperature [8], which are 0.13 for PHEC-40, 0.29 for PTMO-40 and ~1 for PDMS/PHMO-40 [i.e., PDMS segments are completely segregated from the other segments]. Since only a small fraction of hard segments are separated from the soft matrix in PHEC-40, relatively little thermal energy is required for complete hard domain dissolution. The formation of a homogeneous mixed phase involving the PDMS soft segments was initially surprising, considering that the solubility parameters [34] of the PDMS and hard segments are significantly different

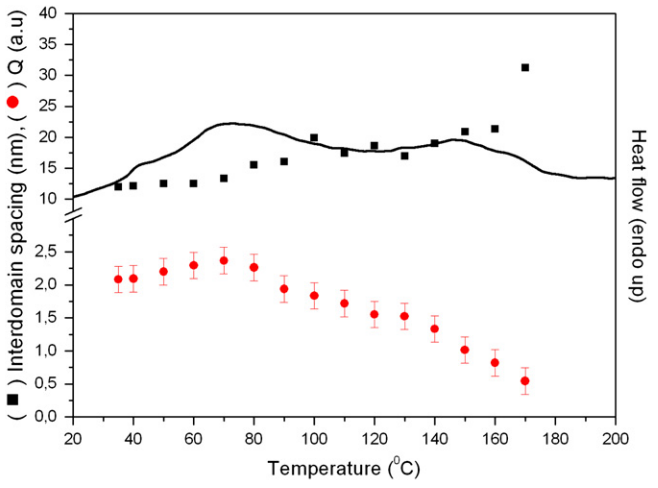

**Fig. 11.** Experimental interdomain spacings (■) and $Q$ (●) for PTMO-40 as a function of temperature, overlaid with the DSC thermogram (heating rate = 10 °C/min) of a sample with the same thermal history as that used for the SAXS experiment.

(11.9 ± 0.4 (cal/cm$^{-3}$)$^{1/2}$ and (6.7 (cal/cm$^{-3}$)$^{1/2}$) and no intersegment hydrogen bonding is possible. The complete mixing at elevated temperatures clearly arises and PDMS, respectively). Hence, from the dominance of the entropy of mixing over the unfavorable enthalpic contributions, favored in this case since the PDMS and mean hard segment sequence lengths are relatively small.

One of the factors influencing the microphase separation of segmented polyurethanes is the hard-segment length distribution [16]. This is equivalent for the three copolymers under consideration and the differences in the temperature dependent hard domain dissolution must arise from the different hard/soft segment miscibility. To illustrate our findings more clearly, the SAXS interdomain spacing, $d$, and invariant are displayed in Figs. 10–12, along with the DSC thermogram of each obtained at the same heating rate as that used in the synchrotron SAXS experiments.

For PDMS/PHMO-40 (Fig. 10), the sharp increase in the interdomain spacing at temperatures above 120 °C is near the onset of the DSC endotherm of the PDMS/PHMO-40 copolymer having the

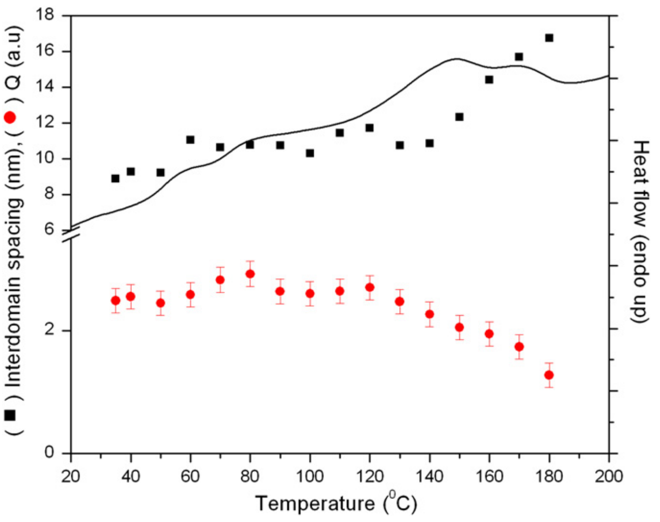

**Fig. 10.** Experimental interdomain spacings (■) and $Q$ (●) for PDMS/PHMO-40 as a function of temperature, overlaid with the DSC thermogram (heating rate = 10 °C/min) of a sample with the same thermal history as that used for the SAXS experiment.

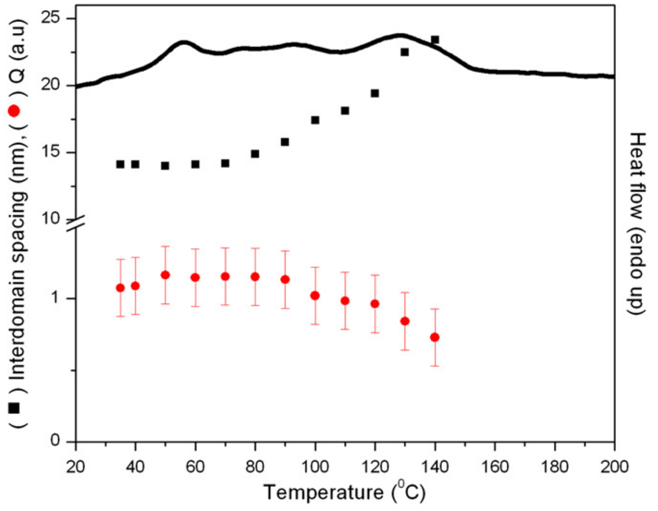

**Fig. 12.** Experimental interdomain spacings (■) and Q (●) for PHEC-40 as a function of temperature, overlaid with the DSC thermogram (heating rate = 10 °C/min) of a sample with the same thermal history as that used for the SAXS experiment.

same thermal history [9], and the endotherm concludes near the temperature where the SAXS intensity disappears. As the PU copolymers under consideration do not exhibit any crystallinity with the preparation used here, these results lead to the conclusion that hard domain dissolution is atleast partially, perhaps completely, responsible for the observed DSC endotherm at these temperatures. There are two small events around 50 and 80 °C in the thermogram in Fig. 10, and it is not immediately clear if one or both of these are endotherms or associated with a change in heat capacity indicative of a $T_g$. In light of our previous discussion, it seems likely however that the higher temperature event is associated with about $T_{g,H}$. A small increase in mean interdomain spacing accompanies the event at 50 °C (and changes in hydrogen bonding are also observed at this temperature in the FTIR experiments discussed earlier), but this is insufficient to assign the origin of this event.

The DSC thermogram and the SAXS interdomain spacings and invariants are displayed for the PTMO-40 copolymer in Fig. 11. A sharp increase in $d$ at temperatures above 120 °C is commiserate with the onset of the higher temperature DSC endotherm and the endotherm concludes near the temperature where the SAXS intensity disappears (above ~170 °C). These results again demonstrate that this endotherm is associated with dissolution of the hard domains. Near the maximum of a lower temperature DSC endotherm, $Q$ begins its gradually decrease, and the interdomain spacing increases before leveling off prior to the second endotherm. As endotherms are commonly associated with the change in heat capacity at $T_g$ due to enthalpy relaxation, it seems reasonable that atleast part of the observed thermal event near 70–80 °C is associated with the $T_g$ of hard domains.

Likewise, $Q$ gradually decreases and the interdomain spacing increases sharply at temperatures above 80 °C for PHEC-40 (Fig. 12), which is coincident with a complex series of endotherms that atleast partially originate from dissolution of hard domains. In keeping with the low degrees of hard/soft segment phase separation for PUs containing 1 K molecular weight PHEC soft segments [8] the scattering peak for PHEC-40 disappears above ~40 °C, a significantly lower temperature than those observed the for PDMS/PHMO-40 and PTMO-40 copolymers.

## 4. Summary

The temperature dependent SAXS characteristics for the PHEC-40, PTMO-40 and PDMS/PHMO-40 PU copolymers were found to be qualitatively similar: an initial increase in $[Q_T/Q_{T_0}]^{1/2}$ is followed by a gradual reduction with increasing temperature. The initial increase likely arises from differential thermal expansion of the hard and soft phases, and the subsequent higher temperature decrease with relatively gradual dissolution of the hard domains. FTIR spectral changes with increasing temperature are also qualitatively similar for the copolymers, and the observed decrease in hard segment hydrogen bonding with increasing temperature is in keeping with the SAXS results and indicates a greater degree of mixing between hard and soft segments at higher temperatures.

There is generally a sharp increase in SAXS interdomain spacing in the higher temperature region where a DSC endotherm is observed, and along with the reduction in $Q$, supports the assignment of this endotherm to dissolution of hard domains. For all copolymers investigated here, the conclusion of this endotherm occurs at a very similar temperature to that at which the SAXS intensity disappears, i.e., the microphase mixing temperature. The $T_{MMT}$ occurs at slightly lower temperatures for the PTMO copolymer compared to PDMS/PHMO-40, while that for PHEC-40 was found to be considerably lower, in keeping with the significantly great solubility of the PHEC and hard segments.

## Acknowledgments

The authors would like to express their appreciation to Dr. John Pople and his colleagues at the Stanford Synchrotron Radiation Laboratory for their kind support and cooperation in the use of SSRL beamline 1–4. We would also like to thank the NSF Polymers Program, through DMR-0605627 and DMR- 0907139, for partial support of this research.

## References

[1] Peebles LH. Macromolecules 1976;9:58.
[2] Koberstein JT, Galambos AF. Macromolecules 1992;25:5618–24.
[3] Christenson CP, Harthcock MA, Meadows MD, Spell HL, Howard WL, Creswick MW, et al. J Polym Sci Part B Polym Phys 1986;24:1401–39.
[4] Ginzburg VV, Bicerano J, Christenson CP, Schrock AK, Patashinski AZ. J Polym Sci Part B Polym Phys 2007;45:2123–35.
[5] Garrett JT, Runt J, Lin JS. Macromolecules 2000;33:6353–9.
[6] Koberstein JT, Stein RS. J Polym Sci Part B Polym Phys 1983;21:1439–72.
[7] Choi T, Weksler J, Padsalgikar Ajay, Runt J. Polymer 2009;50:2320–7.
[8] Hernandez R, Weksler J, Padsalgikar A, Choi T, Angelo E, Lin JS, et al. Macromolecules 2008;41:9767–76.
[9] Hernandez R, Weksler J, Padsalgikar A, Runt J. Macromolecules 2007;40:5441–9.
[10] Garrett JT, Siedlecki CA, Runt J. Macromolecules 2001;34:7066–70.
[11] Li YJ, Gao T, Chu B. Macromolecules 1992;25:1737–42.
[12] Saiani A, Novak A, Rodier L, Eeckhaut G, Leenslag JW, Higgins JS. Macromolecules 2007;40:7252–62.
[13] Desper CR, Byrne CA, Li Y, Chu B. Macromolecules 1995;28:4213–26.
[14] Koberstein JT, Russell TR. Macromolecules 1986;19:714–20.
[15] Leung LM, Koberstein JT. Macromolecules 1986;19:706–13.
[16] Cooper SL, Miller JA, Lin SB, Hwang KKS, Wu KS, Gibson PE. Macromolecules 1985;18:32–44.
[17] Saiani A, Daunch WA, Verbeke H, Leenslag JW, Higgins JS. Macromolecules 2001;34:9059–68.
[18] Saiani A, Rochas C, Eeckhaut G, Daunch WA, Leenslag JW, Higgins JS. Macromolecules 2004;37:1411–21.
[19] Gunatillake PA, Meijs GF, McCarthy SJ, Adhikari R. J Appl Polym Sci 2000;76:2026–40.
[20] Gehrke R, Riekel C, Zachmann HG. Polymer 1989;30:1582–90.
[21] Li YJ, Gao T, Liu J, Linliu K, Desper CR, Chu B. Macromolecules 1992;25:7365–72.
[22] Choi T, Weksler J, Padsalgikar A, Runt J, in preparation.
[23] Martin DJ, Warren LAP, Gunatillake PA, McCarthy SJ, Meijs GF, Schindhelm K. Biomaterials 2000;21:1021–9.
[24] Coleman MM, Lee KH, Skrovanek DJ, Painter PC. Macromolecules 1986;19:2149–57.
[25] Skrovanek DJ, Painter PC, Coleman MM. Macromolecules 1986;19:699–705.
[26] Yilgor I, Yilgor E, Guler IG, Ward TC, Wilkes GL. Polymer 2006;47:4105–14.
[27] Sheth JP, Wilkes GL, Fornof AR, Long TE, Yilgor I. Macromolecules 2005;38:5681–5.
[28] Christenson EM, Dadsetan M, Wiggins M, Anderson JM, Hiltner A. J Biomed Mater Res Part A 2004;69A:407–16.
[29] Joseph MD, Savina MR, Harris RF. J Appl Polym Sci 1992;44:1125–34.
[30] Krevelen DWV. In: Properties of polymers. 3rd ed. Elsevier; 1997.
[31] Orwoll RA. In: Physical properties of polymers handbook. 2nd ed. Springer; 2007.
[32] Lee H, Fragiadakis D, Castagna AM, Runt J, in preparation.
[33] Chen TK, Chui JY, Shieh TS. Macromolecules 1997;30:5068–74.
[34] Coleman MM, Graf J, Painter P. Specific interactions and the miscibility of polymer blends. Lancaster: Technomic Publishing; 1991.